# Full-duplex Metamaterial-enabled Magnetic Induction Networks in Extreme Environments

Hongzhi Guo and Zhi Sun

Department of Electrical Engineering, State University of New York at Buffalo, Buffalo, NY 14260

E-mail: {hongzhig, zhisun}@buffalo.edu.

*Abstract*—**Many important applications in the extreme environment require wireless communications to connect smart devices. Metamaterial-enhanced magnetic induction ($M^2I$) has been proposed as a promising solution thanks to its long communication range in the lossy medium. $M^2I$ communication relies on magnetic coupling, which makes it intrinsically full-duplex without self-interference. Moreover, the engineered active metamaterial provides reconfigurability in communication range and interference. In this paper, the new networking paradigm based on the reconfigurable and full-duplex $M^2I$ communication technique is investigated. In particular, the theoretical analysis and electromagnetic simulation are first provided to prove the feasibility. Then, a medium access control protocol is proposed to avoid collisions. Finally, the capacity and delay of the full-duplex $M^2I$ network are derived to show the advantage of the new networking paradigm. The analysis in this paper indicates that in a full-duplex $M^2I$ network, the distance between the source and destination can be arbitrarily long and the end-to-end delay can be as short as a single hop delay. As a result, each node in such network can reach any other node by one hop, which can greatly enhance the network robustness and efficiency. It is important for timely transmission of emergent information or real-time control signals.**

## I. INTRODUCTION

Wireless communications in extreme environments, e.g., underwater and underground, emerged in early 20th century [1] driven by military and industrial applications. Extremely large electric/magnetic antennas that can overcome the high absorption loss are installed on submarines for underwater surveillance or employed by miners for underground exploration. During the past two decades, the development of wireless sensor/robotic network offers another solution that all the activities in hostile and dangerous extreme environments can be done automatically without human intervention. However, the sensors and robots are much smaller than a submarine and the conventional technologies cannot be directly adopted. Therefore, the extreme environment wireless network requires low-profile and high-efficiency communication technologies.

The magnetic induction (MI) communication relying on loop antenna coupling is an efficient solution in extreme environments thanks to its small penetration loss and stable wireless channel [2]–[4]. It has been extensively utilized for wireless communication and wireless sensing in underground, underwater, and food logistics [2], [5], [6]. Since its operating frequency is relatively low (High Frequency band or lower), it is impossible to design an efficient antenna with the desired low profile. Motivated by this, the metamaterial-enhanced

magnetic induction ($M^2I$) communication is proposed and implemented in [7], [8] which can achieve long communication range by using low-profile antenna (10 cm in diameter). Metamaterial is a kind of periodical artificial structure that can significantly change the wave propagation [9], [10]. To date, the understanding of $M^2I$ is still limited to point-to-point communications.

In this paper, we investigate an important but yet untouched property of the $M^2I$-based wireless network, i.e., the *full-duplex* capability. In particular, $M^2I$ is based on near field coupling and the relay is intrinsically full-duplex: since the received signal at the relay node can generate a new time-varying magnetic field from the coil antenna, the relay node actually re-broadcasts the received signal immediately after receiving it. While the self-interference creates numerous problems and remains the key challenges in the full-duplex design in conventional electromagnetic (EM) wave-based networks, the full-duplex $M^2I$ relay does not suffer from any self-interference. The full-duplex $M^2I$ relay actually share the same principle as the transformer, which also relay the electricity in a full-duplex manner.

It should be noted that the existing $M^2I$ technique [7], [8] is based on passive metamaterial thus the gain at the relay node is fixed and not enough for long-range full duplex relay. To enable the flexible control of the full-duplex relay and extend the relay range in $M^2I$-based network, we propose to use active metamaterial instead of passive one. Recently, active elements have been introduced to metamaterial to overcome its loss, broaden its bandwidth, and, more importantly, make it reconfigurable [11]. By adding such active elements into the existing $M^2I$ antennas, the gain of the full-duplex relay can be greatly enhanced and arbitrarily controlled. As a result, a $M^2I$ full-duplex relay can be turned on or off; and the relay coverage range can also be controlled, in real time.

In this paper, we answer three key questions in the full-duplex $M^2I$ networks: (i) how to realize and control the full-duplex $M^2I$ relay node? (ii) how to avoid the high interference caused by the large full-duplex relay area? and (iii) what is the network capacity and end-to-end delay in such network? Specifically, the operation framework of the reconfigurable full-duplex $M^2I$ network is first introduced and its unique characteristics are emphasized. Then, we reduce the complexity of the $M^2I$ antenna model and provide a feasible active input design. Based on simplified model, the controllable metamaterial gain is analyzed and the stable condition of the active input is found. Moreover, the full wave EM simulation is conducted to verify the feasibility of the active

reconfigurable $M^2I$ relay. After that, the link budget model is derived with reconfigurable metamaterial gain and full-duplex relay. In addition, we design a practical medium access control (MAC) protocol to efficiently realize the proposed network framework, upon which the network capacity and delay models are developed. Through numerical simulation, we prove the feasibility and stability of the $M^2I$ network. The low-delay performance is also verified.

The reminder of this paper is structured as follows. Section II gives the fundamental background of the reconfigurable full-duplex $M^2I$ relay. Then, the system model is introduced in Section III. Based on it, the link budget, network protocol, and network capacity and delay are analyzed in Section IV. Numerical simulations are provided in Section V. Finally, we conclude this paper in Section VI.

## II. $M^2I$ Full-duplex Multihop Network

The multihop relay has been widely used in conventional EM wave-based wireless networks to overcome the limitation of short communication range. However, since the self-interference problem [12] has not been perfectly addressed so far, the half-duplex multihop mechanism [13] significantly increases the end-to-end delay from the data source to the destination. For example, a packet is sent from node $N_1$ to $N_n$ through relays $N_2$ to $N_{n-1}$. Assume that it takes $T_0$ for one hop and thus the minimum end-to-end transmission delay without interference from other simultaneous transmissions is $(N_n - 1)T_0$.

In contrast, $M^2I$-based wireless network can achieve full-duplex multihop relay without the impact of self-interference. As a result, the source node and destination node can be arbitrarily far apart from each other as long as there are enough relay nodes in-between. Since all the relays are full-duplex, the delay will be $T_0$ rather than $(N_n - 1)T_0$ in the aforementioned scenario. That is to say, the end-to-end delay of the multihop transmission in full-duplex $M^2I$ network can be as short as one transmission duty cycle. Each node in such network can reach any other node by just one hop, which can greatly enhance the network robustness and efficiency. It is a dramatical departure from the current multihop networking mechanisms and is very important for timely transmission of emergent information for sensor networks or real-time control signals for robotic networks in extreme environments.

The reason why the full duplex $M^2I$ network does not suffer from self-interference can be explained as follows.

In EM-based communication, the wireless devices are placed many wavelengths away. When the transmitter sends a packet to the receiver, the relay can overhear it since the EM wave can induce currents in its antenna. This induced current can be regarded as a re-radiation source that is broadcasting the received signal by the relay into the space. However, this signal cannot be received by the receiver due to two reasons. First, the induced current in the relay's antenna is weak since the range between the transmitter and the relay is large when compared with wavelength. Moreover, the receiver is also far from the relay. As a result, the reradiated signal cannot be captured by the receiver and the relay has to send the packet again after it receiving the packet. For full-duplex EM relay, since
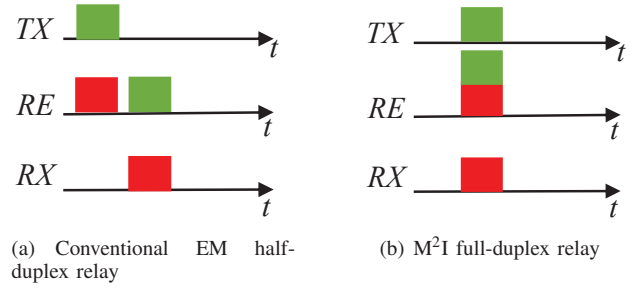


(a) Conventional EM half-duplex relay

(b) $M^2I$ full-duplex relay

Fig. 1. Comparison of conventional relay and $M^2I$ relay. The green block is a transmitted packet and the red block is a received packet.

it transmits and receives simultaneously, the self-interference is a great challenge and usually the performance has to be sacrificed when uses full-duplex relay [12], [14].

The $M^2I$ is a different technology from EM communication because it employs the near field radiated by magnetic loop antennas [2], [3], [7], [15]. As a result, the transceivers in $M^2I$ communication networks have a much stronger coupling (mutual interaction) and the information can be delivered via this coupling. Different from the EM relay, the $M^2I$ relay is intrinsically full-duplex thanks to the near filed coupling. Consider that a $M^2I$ relay is located between the transmitter and receiver, the transmitted signal can induce currents in the relay, which is the same as the EM wave. The difference is that the relay with induced current can be regarded as a new radiation source. Since the coupling between the receiver and the relay is strong, the relay can also induce currents, carrying the transmitted signal, at the receiver. All the above processes happen simultaneously due to the relatively short communication range and strong magnetic coupling.

An example is provided in Fig. 1. For EM half-duplex relay, the transmitter sends a packet, which is received by the relay and forwarded to the receiving node in the next time slot. Therefore, the transmission process consumes two time slots. On the contrary, in the full-duplex $M^2I$ networks, only one time slot is required to complete the data transmission. As shown in Fig. 1(b), the relay and receiving nodes get the packet simultaneously. Originally, the transmitter cannot communicate directly with the receiver due to the long distance between them. Now, the full-duplex relay can improve the coupling strength among the three nodes and the packet can be delivered immediately to the receiver.

## III. Modeling Full-duplex $M^2I$ Network

In this section, we develop succinct analytical model for reconfigurable $M^2I$ communication and networking.

### A. Characteristics of $M^2I$ Communication

*1) $M^2I$ Enhancement:* In [7], [8], the fundamental electromagnetic principles of $M^2I$ is analyzed by considering an ideal model with homogeneous and isotropic metamaterial, which is followed by a practical design and implementation using a spherical coil array. The results show that the metamaterial provides a gain $\alpha_{gain}$ for radiated magnetic field and self-inductance, while the mutual inductance is increased by $\alpha_{gain}^2$, where $\alpha_{gain}$ can be controlled by the metamaterial parameters,
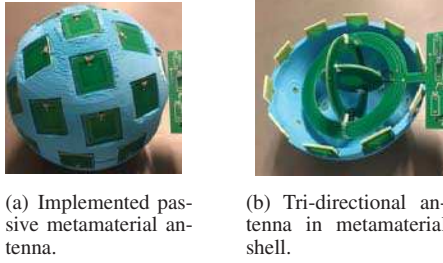
(a) Implemented passive metamaterial antenna.

(b) Tri-directional antenna in metamaterial shell.

Fig. 2. Passive metamaterial-enhanced magnetic antenna.



Fig. 3. Metamaterial unit with reconfigurable NIC.

such as thickness, effective permeability, and loss. For example, if the radiated magnetic field by a MI antenna is $H_m$, the antenna self-inductance is $L_m$, and the mutual inductance between two MI transceivers is $M_m$, then the corresponding parameters for M$^2$I will be $\alpha_{gain}H_m$, $\alpha_{gain}L_m$, and $\alpha_{gain}^2 M_m$, respectively.

Since the developed model in [7], [8] is comprehensive, it is so complicated that cannot be directly adopted. Next, we first provide a simplified model for $\alpha_{gain}$ and then we prove that it is reconfigurable. The original self-inductance of a loop antenna can be written as

$$L_{MI} = \frac{\Phi_{MI}}{I_{MI}} = \frac{\mu N_t H_{MI} S_a}{I_{MI}}, \tag{1}$$

where $\Phi_{MI}$ is the magnetic flux across the MI antenna, $I_{MI}$ is the current, $H_{MI}$ is the radiated magnetic field in the vicinity of the antenna, $N_t$ is the number of turns, $\mu$ is the permeability, and $S_a$ is the area of the antenna. When the antenna is enclosed by the metamaterial shell, the enhanced self-inductance can be written as

$$L_{M^2I} = \frac{\Phi_{M^2I}}{I_{M^2I}} = L_{MI} - \Re\left[\sum_{i=1}^{N_{meta}} \frac{j\omega\{M_{am}\}_i^2}{Z_r + j\omega L_{mu} + \frac{1}{j\omega C_{mu}} + \Im(Z_{ref})}\right], \tag{2}$$

where the second term on the right-hand side is caused by the metamaterial shell, $Z_r = R_{mu} + R_{active} + \Re(Z_{ref})$, $\Phi_{M^2I}$ is the magnetic flux through the loop antenna, $I_{M^2I}$ is the antenna current, $N_{meta}$ is the number of metamaterial units on the shell, $R_{mu}$ is the resistance of the metamaterial unit, $R_{active}$ is the active input resistance which is reconfigurable, $L_{mu}$ is the self-inductance of a metamaterial unit, $C_{mu}$ is the capacitance in metamaterial unit, $\{M_{am}\}_i$ in the mutual inductance between the antenna and the $i^{th}$ metamaterial unit, $Z_{ref}$ is the reflected impedance from other metamaterial units to the $i^{th}$ unit, which is the same for all the units since the units are uniformly distributed on the spherical shell, and $\Re(\cdot)$ and $\Im(\cdot)$ stands for the real and imaginary part of a complex number, respectively.

Therefore, the gain of metamaterial enhancement can be expressed as

$$\alpha_{gain} = \frac{L_{M^2I}}{L_{MI}}. \tag{3}$$

By using different configurations in (2), this gain can be adjusted [7], [8].

### B. Reconfigurable M$^2$I Antenna Model

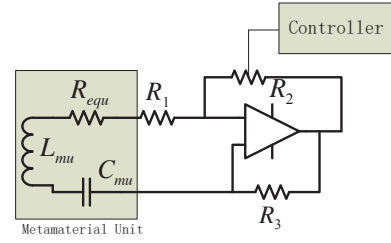In Fig. 2, a M$^2$I prototype is fabricated with passive metamaterial elements and a tri-directional antenna with three mutually perpendicular unidirectional coils are placed in the center of the shell to overcome the polarization loss. Such a passive metamaterial shell is easy to fabricate, but it is not trivial to make it reconfigurable due to its complicated structure. Next, we provide a solution to design reconfigurable active metamaterial based on negative impedance converter (NIC).

The Non-Foster Element (NFE) has been extensively utilized in antenna and amplifier impedance matching, oscillators, and low-loss metamaterial design since it can demonstrate negative resistance, self-inductance, or capacitance. The NIC is employed to create effective NFE, e.g., in Fig. 3 the equivalent impedance is a negative resistance [16], [17]. The NIC is connected in series with the metamaterial unit, i.e., the small PCB in Fig.2(a). In view of (2) and (3), the resistive losses in the metamaterial units, i.e., $R_{mu}$ and $Z_{ref}$ in (2), affect the gain dramatically. By using the NFE, a negative resistance $R_{active}$, can be created to compensate the loss with active DC power input. Although the gain can be enhanced, this method also introduces two negative effects: stability issue and additional noise. The negative impedance need to be designed to meet the stability condition, otherwise unpredictable and infinitely large current can be generated [18]. Moreover, the resistive elements in the NIC also introduces noises that can corrupt signals. In the following, we discuss the gain and the two negative effects in sequence.

*1) Reconfigurable Gain:* By using a reconfigurable $R_2 = \{R_{rcfg}[i]\}_{i=1}^{N_{tap}}$, the negative resistance $R_{active}$ can be digitally controlled by the central controller, e.g., using a digital potentiometer. As a result, the resistive elements in a metamaterial unit can be expressed as

$$\{Z_r[i]\}_{i=1}^{N_{tap}} = R_{mu} + \Re(Z_{ref}) - \frac{\{R_{rcfg}[i]\}_{i=1}^{N_{tap}}}{R_1}R_{ref}. \tag{4}$$

Then, by substituting (4) into (2) and (3), we can obtain the reconfigurable gain $\{\alpha_{gain}[i]\}_{i=1}^{N_{tap}}$.

*2) Stability:* In the following, we provide an analytical understanding of the instability of active metamaterial and derive the stable condition that needs to be satisfied. As discussed in [8], $\alpha_{gain}$ is achieved when the metamaterial unit's reactance is negative which is equivalent to a capacitor. Then, the equivalent circuit of the metamaterial unit can be simplified to a positive resistor $R_{equ} = R_{mu} + \Re(Z_{ref})$, a capacitor $C_{equ}$, and the negative resistor $R_{active}$. The Laplace Transform of the induced current in a metamaterial unit is given by

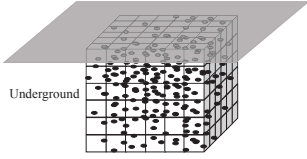$$I_{mu} = \frac{\mu H_{mu} S_a s}{1/(C_{equ}s) + R_{equ} + R_{active}}. \tag{5}$$

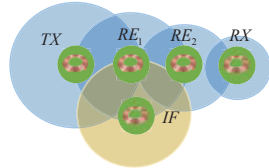Fig. 4. Cell partition of underground sensor networks. Black dots are sensor nodes.



Fig. 5. Interference in M²I relay. Colored disk is the communication range.

To satisfy the Routh stability criterion, $R_{equ} + R_{active}$ should be larger than 0. As a result, the stable condition is

$$R_{active} > -R_{equ}. \qquad (6)$$

Under this condition, the induced current in the metamaterial unit is finite and thus the system becomes stable, otherwise infinite current can be induced.

*3) NIC Noise:* By using the NIC, more noises are introduced to the system, which may equivalently change the effective value of $R_{active}$. In this paper, we model the noise of NIC as the thermal noise generated by $R_{active}$, i.e., $v_{nic} = \sqrt{-4k_B T R_{active} B_w}$, where $k_B$ is the Boltzmann's constant, $T$ is the temperature, and $B_w$ is the bandwidth. Similarly, given $R_{mu}$, we can obtain the generated noise voltage. The noises force the metamaterial units to radiate power and induce voltage in the loop antenna, which is considered as the reflected noise in the loop antenna that can corrupt the received signal.

*C. Network Model*

The terrestrial wireless networks spans in a 2D space and thus most of the analysis considers 2D scenario. However, most of the extreme environments are 3D, e.g., underground sensor networks and underwater robotic networks. Hence, in this paper we consider a 3D network, which is different from the existing works.

*1) Topology and Interference Model:* The cell partition is widely used in 2D network analysis [19]. Here, we extend it to 3D by considering an ad-hoc network with uniformly distributed node in a 3D cube with edge length $l_s$. The node density is $\lambda_n$ and node $i$'s position is denoted by $X_i$. In addition, we divide the space into small sub-cubes with edge length $l_{sc}$ as shown in Fig. 4. Note that the environment is not necessary to be underground, it can be many other extreme and complex environments. This cubic structure can find many applications in realistic. For example, in [6], the MI sensors are placed in boxes on a food truck to monitor the food quality in real time; in underwater fish farming, fishes are fostered in cages, which are organized in a similar way as the proposed network structure; the MI sensors/robots can be placed in the cage to collect useful information.

The extensively used protocol model [20] is considered for adjacent node interference. Assume that the communication range associated with gain $\alpha_{gain}[i]$ is $d_{max}[i]$, where $i = 1, 2, \cdots N_{tap}$. A link can achieve a data rate of $\mathcal{R}$ only if all the interferers are $(1 + \Delta)d_{max}[i]$ away from the receiver.

The routing strategy employs the shortest path from the source to the destination. The nodes in a cell can communicate with all the nodes in its neighbor cells. As a result, the route from the source to the destination is the line connecting

them if there is no empty cells. In existing works, there is a relation of the node density, cell size, and communication range that can guarantee all the cells contain at least one node [20]–[22]. However, this condition is hard to be satisfied in MI communication networks because of the relatively short communication range, which requires extremely large numbers of nodes in a small area. Therefore, in this paper we consider the scenario that the network is connected but empty cells are allowed. In the routing algorithm, each node checks its neighbor and choose the one which is not empty and has the shortest distance to the destination as the relay. To make the routing algorithm converge, we use the cells' center to measure the distance between two cells.

*2) Metamaterial Gain Control:* Although the gain provided by the metamaterial can significantly improve the communication range, this also creates more interferences. Therefore, we cannot aggressively increase the gain by sacrificing the network throughput. In addition, an important unique characteristic of the M²I full-duplex relay networks is the interference introduced by relay nodes. For the conventional EM-based half-duplex and full-duplex communication, the interference cannot be directly transmitted from the relay to the destination. However, in M²I full-duplex relay networks, the relay nodes not only deliver useful signals but also the interference signals. For example, in Fig. 5, $RE_1$ and $RE_2$ can relay the signal from $TX$ to $RX$. Since the relays are full-duplex, $RE_1$ and $RE_2$ receive the signal and transmit it immediately. Now, in presence of the interferer $IF$, the interference signal also propagates from $RE_1$ to $RE_2$ and $RX$. However, if $IF$ employs a smaller gain, then $RE_1$ receives less or even no interference. As a result, the throughput can be improved. In next section, we provided a solution to control the metamaterial gain for each device to achieve higher throughput while maintain the communication link.

IV. FULL-DUPLEX M²I NETWORK ANALYSIS

In this section, we derive the link budget model for full-duplex M²I network, upon which the single transmission in the network is analyzed. After that, we provide a MAC protocol and analyze the network performance with multiple transmissions.

*A. Link Budget for Full-duplex M²I Relay*

*1) Mutual Inductance:* The widely used omnidirectional loop antenna can no longer guarantee the coverage in a 3D space, because it only has the same directional property on one plane rather than the whole 3D space [23]. Moreover, the MI communication employs the near field as well as the transition region of the antenna, which makes the analysis far more complicated than the EM communication. Therefore, we need to employ an isotropic antenna to overcome the directional loss in 3D space and derive a simple but rigorous mutual inductance model.

In [5], [24] the tri-directional (TD) antenna with three mutually perpendicular loop antennas is utilized to create isotropic coverage. In this paper, we follow the TD antenna model in [5], where the TD antenna is modeled by using a 3 by 3 orthogonal matrix. As shown in [5], TD antenna can
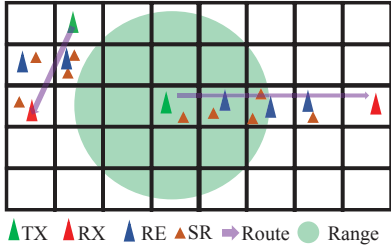
TX ▲ RX ▲ RE ▲ SR ➡ Route ● Range

Fig. 6. A 2D illustration of data transmission in M²I network with relay.

achieve the optimal performance that is equivalent to the well-aligned unidirectional antenna. Different from [5] where the TD antenna is utilized in a stratified medium, here we prove a general case that the TD receiving antenna can always capture the maximum amount of power, which makes it immune to orientation change.

Considering the incident magnetic field as $H_{in} = \mathbf{u}_{in}|H_{in}|$, where $\mathbf{u}_{in}$ is a unit vector denoting the incident direction and $|H_{in}|$ is the magnitude. The orientation of a TD receiving antenna is $\mathbf{R}_{td}^t = [\mathbf{u}_1, \mathbf{u}_2, \mathbf{u}_3]$, where the superscript $t$ means matrix transpose and $\mathbf{u}_i$ is a unit vector. Then, the induced voltage in the TD antenna is $v_{td} = j\omega\mu|H_{in}|S_a\mathbf{u}_{in}\mathbf{R}_{td}^t$. The received power is proportional to $\mathbf{v}_{td} \cdot \mathbf{v}_{td}^t$, which can be expanded as $-\omega^2\mu^2|H_{in}|^2S_a^2\mathbf{u}_{in}\mathbf{R}_{td}\mathbf{R}_{td}^t\mathbf{u}_{in}^t$. Since $\mathbf{R}_{td}^t$ is an orthogonal matrix, $\mathbf{R}_{td} \cdot \mathbf{R}_{td}^t$ equals an identity matrix. As a result, the received power is independent of the TD antenna orientation. In addition, since $\mathbf{u}_{in}$ is a unit vector, $\mathbf{u}_{in} \cdot \mathbf{u}_{in}^t = 1$. Thus, the incident magnetic field can be fully utilized without antenna orientation loss by using the TD antenna.

As a result, we can reduce the negative orientation effect by using the TD antenna in a metamaterial shell. In the following we consider the antennas are well-aligned without any loss from antenna orientation. Next, the mutual inductance is written as a function of the transceivers' distance using TD antennas, upon which we can derive the link budget model. By considering the metamaterial gain, the mutual inductance between two M²I transceivers can be written as [2], [7]

$$M = \frac{N_t^2\mu\alpha_{gain}[i]\alpha_{gain}[j]S_a^2e^{-jkd}f(\theta)}{2\pi d^3} = C_1\frac{\alpha_{gain}[i]\alpha_{gain}[j]}{d^3},$$ (7)

where $d$ is the distance between the M²I transceivers, $k$ is the propagation constant, and $f(\theta)$ stands for the orientation effect. Since the TD antenna's three unidirectional coils are mutually perpendicular to each other, they can radiate fields into arbitrary direction when they are connected in series. Also, the transmitting TD antenna is almost isotropic in the near field [5], [23]. In the following, we consider the mutual inductance between two transceivers is the maximum value without orientation effect, i.e., $f(\theta) = 1$ in (7).

*2) Link Budget for Single Transmission:* According to the routing strategy introduced in Sec. III-C1, there is a path from the source to the destination and each cell on the path has at least one node. We assume that there are $N_c$ cells along the path. Moreover, each node, including the relay can adjust their metamaterial gain based on local observations of the network status, such as interference and connection. The

required data rate is $\mathcal{R}$ and either with or without relay the minimum received Signal-to-Noise Ratio (SNR) should be larger than $2^{\mathcal{R}} - 1$. When there is no relay, the transmitter can directly send data to the receiver and the path loss can be modeled as [2], [25]

$$\mathcal{L} = -10\log_{10}\left[\frac{\omega^2M^2}{2(R_{M^2I}^2 + \omega^2M^2)}\right],$$ (8)

where $R_{M^2I}$ is the resistance of the M²I antenna. Note that the path loss model is different from the one in [26] which neglects the term $\omega^2M^2$ on the denominator. Since the metamaterial can significantly increase the mutual coupling, if we neglect this term on the denominator, the path loss can be smaller than 0, which is not true. If $M$ is large enough, the minimum $\mathcal{L}$ is 3 dB which means only half of the transmission power can be delivered to the receiver and the other part is dissipated in the transmitter. When there are $N_c$ relays in between the transmitter and receiver, due to the long communication range, there are significant propagation losses. Therefore, to achieve the required data rate, the transmitter and relays have to be coupled much stronger, i.e., smaller path loss for each hop. Thus, there is a limitation on the path loss of each hop which will be given in the following part. The path loss with relay can be written as

$$\mathcal{L}_{relay}^{N_c} = -10\log_{10}\left[\prod_{i=1}^{N_c+1}\frac{\omega^2M_i^2}{2(R_{M^2I}^2 + \omega^2M_i^2)}\right]$$

$$= -10\log_{10}\left[\prod_{i=1}^{N_c+1}\frac{\omega^2C_1^2\alpha_{gain}[i]\alpha_{gain}[i+1]}{2\left(R_{M^2I}^2d_i^6 + \omega^2C_1^2\alpha_{gain}^2[i]\alpha_{gain}^2[i+1]\right)}\right].$$ (9)

Here, only the interactions between adjacent neighbors are considered and the nonadjacent interactions are neglected due to the long distance [2], [3].

*B. Single Transmission in M²I Network*

In this subsection, we analyze the cooperative strategy of M²I relay in a single transmission where a source sends data to a destination with relays. Only one active link is considered here and the discussion is extended to multiple active links in a network in the next subsection. Note that the data transmission process consists of two procedures, i.e., relay scheduling and data transmission. The relay scheduling utilizes negligible short time slots to schedule the relays and the associated metamaterial gain. During relay scheduling, each node receives signals from the previous node and decides whether it can serve as a relay or not. If available, it will choose the metamaterial gain based on its received signal strength. If not available, it will keep silent and the previous node will wait for a predefined time slot and then send feedback to the source.

No matter how many relays are employed, the path loss between the transmitter and receiver has to be lower than a threshold to achieve the required data rate $\mathcal{R}$. Although the larger $\alpha_{gain}$ can provide strong couplings, it also creates large interference for other transmissions in the network. Therefore, by meeting the data rate requirement, the interference has to be minimized. Since the interference area $(1 + \Delta)d_{max}$ is

proportional to the communication range $d_{max}$ and $\alpha_{gain}$, we try to minimize the sum of $\alpha_{gain}$ and the problem can be stated as

$$\min \sum_{i=1}^{N_c} \alpha_{gain}[i]$$

$$s.t. \ \mathcal{L}_{relay}^{N_c} = \hat{\mathcal{L}}_{max} \qquad (10)$$

where $\hat{\mathcal{L}}_{max}$ is the maximum path loss that can achieve $\mathcal{R}$. The above problem is nonlinear and requires significant computation to find the optimal metamaterial gain for each node. Also, the information exchange poses high burdens for wireless sensors/robots operating in extreme environments. Here we propose a low complexity solution, where each node can choose its gain based on the received signal strength from the previous node without considering interference control. Each relay node receives signals from the previous relay or source and it has the knowledge of the transmission power. For the $i^{th}$ hop, let the path loss be $\mathcal{L}_i$ when the relay's gain $\alpha_{gain}[i+1] = 1$, i.e., no metamaterial gain. Then, the relay can choose its gain to change the path loss to $\tau\mathcal{L}_i$, where $\tau \leq 1$ and it is a constant. The expression of $\alpha_{gain}[i+1]$ is

$$\alpha_{gain}[i+1] = \frac{2\pi d_{i,i+1}^3 R_{M^2I}}{\omega\alpha_{gain}[i]N_t^2\mu S_a^2|e^{-jkd}|}\sqrt{\frac{0.5C_2}{1-0.5C_2}}, \qquad (11)$$

where $C_2 = 10^{-\frac{\tau\mathcal{L}_i}{10}}$. By changing the $i^{th}$ relay's gain, the path loss can be reduced and the level is determined by $\tau$. When $\tau = 1$, $\alpha_{gain}[i+1] = 1$ and there is no improvement in received signal strength. Therefore, $\tau$ has to be smaller than 1. Based on (11) we can find the interference area whose radius $d_{if}$ is larger than $(1 + \Delta)d_{ifmin}$, where $d_{ifmin}$ is the communication range with both the transmitting gain and the receiving gain equal 1. In addition, $d_{if}$ is smaller than $(1 + \Delta)d_{ifmax}$, where $d_{ifmax}$ is the communication range with transmitting gain and receiving gain is the maximum $\alpha_{gain}$. Based on this relation, we can estimate the interference area.

The single transmission is equivalent to the scenario that the network load is extremely small and the transmission do not suffer from interference. If so, by ideally increasing the metamaterial gain, the communication range can be arbitrarily long using dense relays and all the transmissions can be completed in a single hop, which can significantly reduce the delay.

### C. Multiple Transmissions in M²I Network

*1) MAC Protocol Design:* Although for a single transmission in the network the delay is negligible, this is achieved by equivalently increasing the transmission range and reducing the network capacity. As pointed out in [19], [22], there is a tradeoff between network capacity and delay. The short communication range provides a large network capacity but relatively long delay, while long communication range can reduce the delay of a communication link, it may increase the delay for other packets waiting to be transmitted and reduce the overall network throughput. In the following, we provide both a practical MAC protocol and analyze its performance.

We assume the nodes are omniscient and have perfect knowledge of the topology. The data communication mainly
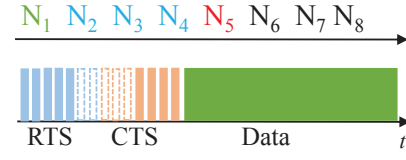

Fig. 7. Modified CSMA/CA for M²I network.

consists of two steps, i.e., random medium access and data transmission. As shown in Fig. 7, the medium access employs very short time slots which can be neglected, while the data packet consumes much more time. First, if the channel is available, the source $S_1$ sends RTS (Request to Send) to the next-hop cell on the path. In the next cell, a node $RE_1$ will voluntarily serve as the relay and adjust its metamaterial gain based on the received power. After that, $RE_1$ sends RTS to the next-hop cell on the path and a node $RE_2$ will voluntarily serve as the relay. This process will continue until at least one of the following happens in a cell: 1) the destination is in the cell, 2) the nodes in the cell are interfered by other transmissions, 3) one node in the cell is relaying packets for other transmissions, and 4) reaching the maximum relay number. The maximum relay number is considered to avoid very long distance transmission because it can dramatically reduce the network capacity. However, if there is an emergent events happening and it has high priority, the network layer can allow large maximum relay number and this will be considered in our future work.

If one of the four conditions is satisfied in a cell $x$, it can be the destination or a relay in that cell. First, if the cell has the destination $D_1$, then it will wait for $(N_{rmax}+1-x)(T_{RTS}+T_{CTS})$, where $N_{rmax}$ is the maximum relay number, $x$ is the hop number from the source, and $T_{RTS/CTS}$ is the time required to send RTS or CTS (Clear to Send), before sending its CTS. Once the node $RE_{x-1}$ receives the CTS from $RE_x$, it will relay this information to the node before it, so on and so forth. When $S_1$ receives the CTS, it will start transmitting and all other relays and destination have been prepared to deliver the packet. Second, if the cell $x$ has a relay and the counter reaches the maximum number of relay, then $RE_x$ will not broadcast a RTS, instead it will send a CTS to the previous relay without waiting. In this scenario, the last relay is considered as a temporary destination, which is not counted into the maximum relay number. During the process, there are at most $(N_{rmax}+1)$ RTS will be transmitted. Since each RTS is associated with a CTS, in the protocol there are $2N_{rmax} + 2$ time slots are reserved for RTS and CTS. If any RTS are dropped due to collision or interference, the scheduling process will stop at the last node sending RTS. CTS will not be interfered thanks to the scheduling process of RTS.

An example is given in Fig. 7. Assume that the maximum relay number is 6, $N_1$ is the source, and $N_8$ is a relay or destination. $N_1$ transmits a packet to $N_8$ and it first sends a RTS to $N_2$. Consider that $N_2$ to $N_5$ are available but $N_6$ is interfered by other transmissions. Then, when $N_5$ sends a RTS to $N_6$, it will not respond. Next, $N_5$ waits for five void time slots, including two RTS and three CTS, and sends a CTS to $N_4$. This process will continue until $N_1$ receives a CTS from $N_2$. After that, it transmits the data packet and $N_2$ to $N_4$ will

serve as full-duplex relay and $N_5$ is the receiver.

*2) Delay and Capacity Analysis:* Since the sources and destinations are uniformly distributed, their distance can be estimated using the following distribution [27]

$$\frac{(L/l_s)^2 - 0.5}{\sqrt{7/60}} \sim \mathcal{N}(0,1), \tag{12}$$

where $\mathcal{N}(0,1)$ is the normal distribution with mean 0 and variance 1. Thus, the average distance from the source to the destination is $L = \sqrt{0.5}l_s$. Based on it we can estimate the number of cells a packet across from the source to the destination. The minimum number of cells is $\lceil L/l_{sc} \rceil$ when the source and destination is in the same row or column. Any other location of the destination will introduce more cells. The maximum number of cells is $3\lceil \sqrt{1/3}L/l_{sc} \rceil$. According to the routing algorithm, the path from the source to the destination can be decomposed into $x, y$, and $z$ direction in Cartesian coordinates and $\sqrt{l_x^2 + l_y^2 + l_z^2} = L$. When $l_x = l_y = l_z$, the total number of cell has the maximum value.

Although we have the bounds for the total number of cells on the path, some of them may be empty. The probability that the cell is empty can be written as $P_{empt} = e^{-\lambda_n l_{ls}^3}$, where $\lambda_n$ is the node density. Although we consider there are empty cells, but $P_{empt}$ is a very small number in order to guarantee that the network is connected. The routing strategy can guarantee that even empty cell exists, the packet can still be delivered to the destination. Therefore, the average distance between the source and the destination is still valid due to the low empty cell ratio.

*a) Delay Analysis:* First, for conventional MI network at most $\lceil \frac{L}{l_{sc}} \rceil$ hops are required to complete the transmission. For each hop, the nodes access the channel using time division to avoid collisions. Since conventional MI does not have reconfigurable gain, its interference area is $4/3\pi(1+\Delta)^3 d_{max}^3[1]$. Only one active transmitter is allowed in this area. So it takes $\lceil 4/3\pi(1+\Delta)^3 d_{max}^3[1]/l_{sc}^3 \rceil T_{data}$ to complete a one-hop transmission and the total average delay in conventional MI network is

$$D_{MI} \leq \lceil \frac{L}{l_{sc}} \rceil \lceil \frac{4}{3l_{sc}^3}\pi(1+\Delta)^3 d_{max}^3[1] \rceil T_{data} \tag{13}$$

For M$^2$I network, the delay depends on the maximum relay number and active source density. If all the relays on the path from the source to the destination are available, only one transmission can complete the process with delay $T_{data}$. Then, the average time delay is

$$D_{M^2I} \leq V_{inf}\lambda_{sc}\lceil \frac{L}{l_{sc}(N_{rmax}+1)} \rceil T_{data}, \tag{14}$$

where $V_{inf}$ is the volume of the maximum interference area. Note that, the shape of $V_{inf}$ depends on the number of relay nodes. When the relay nodes are more than 1, the shape of $V_{inf}$ can be approximated by a cone. When there is no relay nodes, the shape can be approximated by a sphere.

We can understand (13) and (14) from two aspects. First, when the network load is extremely high, i.e., $\lambda_{sc}$ is large, $D_{M^2I} \approx D_{MI}$. Since $\lambda_{sc}$ is large, the M$^2$I transceiver cannot use the full-duplex relay because all its neighbors can be



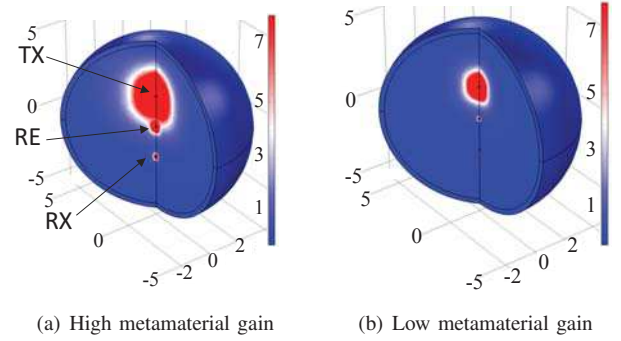(a) High metamaterial gain     (b) Low metamaterial gain

Fig. 8. Simulation of metamaterial gain and interference area. The dimension is measured in meter and the magnetic field is normalized for comparison.

interfered or utilized by other transmissions. Therefore, the number of transmitters within the interference volume is $V_{inf}\lambda_{sc} \approx \frac{4}{3l_{sc}^3}\pi(1+\Delta)^3 d_{max}^3[1]$. Also, when there is no relay, $N_{max} = 0$ which means only the destination receives signal. Second, when the network load is small, i.e., $\lambda_{sc} \approx 0$, $D_{M^2I}$ is much smaller than $D_{MI}$. Under this condition, $V_{inf}\lambda_{sc}$ should be no smaller than 1 to guarantee that there is a transmission. Also, the second term on the right-hand side of (13) is much larger than 1 since $d_{max}[1] \geq \sqrt{5}l_{sc}$ and $\Delta \geq 1$. Since $N_{rmax}$ is much larger than 1, $D_{M^2I}$ is much smaller than $D_{MI}$. This gives us a hint that when there are emergencies which are also rare events (low network load), M$^2$I full-duplex relay network can provide much lower delay.

*b) Network Capacity:* The network capacity $C_{net}$ is defined as the maximum date rate that can be supported from the source to the destination. For conventional MI network, the required throughput from MAC layer is $\lambda_{sc}l_s^3 C_{MInet}\lceil \frac{L}{l_{sc}} \rceil$, while for M$^2$I network the required throughput is $\lambda_{sc}l_s^3 C_{M^2Inet}\lceil \frac{L}{l_{sc}N_{max}} \rceil$ [28]. The maximum number of allowed active link $N_{Lmax}$ is determined by the space reuse and the data rate of each link $\mathcal{R}$. For MI network $N_{Lmax} \leq \lfloor l_s^3/(4/3\pi(1+\Delta)^3 d_{max}^3[1]) \rfloor$. For reconfigurable M$^2$I network $N_{Lmax}$ depends on the metamaterial gain that used by transceivers. If all the transceivers and relays use the minimum gain, $N_{Lmax}$ has the same value as MI. If the transceivers use the maximum gain, $N_{Lmax} \leq \lfloor l_s^3/(4/3\pi(1+\Delta)^3 d_{max}^3[N_{tap}]) \rfloor$. Thus the upper bound of network capacity for MI and M$^2$I network are the same which can be expressed as

$$C_{net} \leq \frac{\mathcal{R}}{\lambda_{sc}l_s^3 \lceil \frac{L}{l_{sc}N_{max}} \rceil}. \tag{15}$$

If the M$^2$I transceivers and relays use larger gain, the active links allowed in the network will reduce.

## V. NUMERICAL SIMULATION

In this section, we numerically analyze the proposed reconfigurable full-duplex M$^2$I network. First, the metamaterial gain is simulated in EM computing software. Then, we analyze the network characteristics, such as node density, empty cells, and communication range of M$^2$I relay. Based on it, the proposed network protocol is simulated.

In Fig. 8, the effect of the metamaterial gain is simulated in COMSOL Multiphysics by using one M$^2$I transmitter (TX),
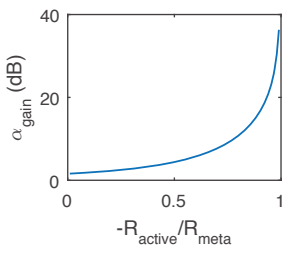
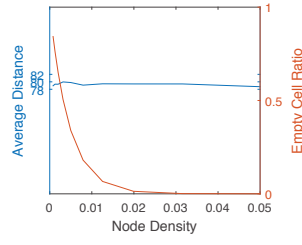Fig. 9. Negative resistance and metamaterial gain.



Fig. 10. Effect of node density on average source-destination distance and empty cell ratio.
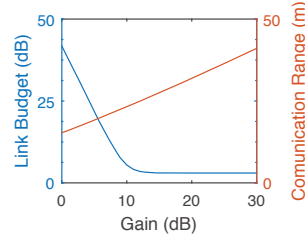


Fig. 11. Link budget between two nodes with different gain and corresponding communication range.
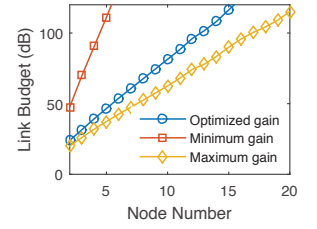


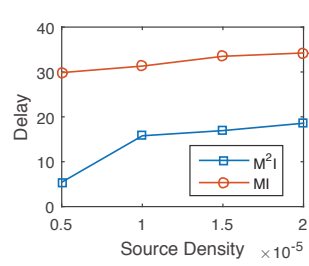Fig. 12. Link budget between source and destination with different relay number.
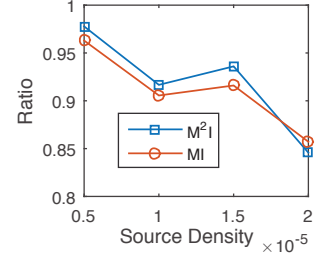


Fig. 13. Average delay. The delay is the number of time slots.



Fig. 14. Average ratio of transmitted packets to total number of packets need to be transmitted in one time slot.

one relay (RE), and one receiver (RX). The configuration of the metamaterial shell and the transceivers is the same as the model in [7]. The considered frequency band is 10 MHz. The interval between the adjacent two nodes is 4 m. As discussed in [8], the metamaterial gain is related to the metamaterial loss, which is the imaginary part of the effective permeability. In Fig. 8(a), the metamaterial equivalent permeability is $-1-0.001j$ which is equivalent to the high metamaterial gain, while in Fig. 8(b), the metamaterial equivalent permeability is $-1-0.01j$ which is equivalent to low metamaterial gain. The red color is the area where the radiated field is above $8 \times 10^{-5}$ A/m (it can be considered as interference area). As shown in the figure, with large metamaterial gain, the relay is more powerful and the receiver can obtain more power. However, the interference area is larger. By dynamically controlling the metamaterial gain, we can freely adjust the transceiver's and relay's coupling to achieve different network performance. In Fig. 9, the effect of the negative resistance on the metamaterial gain is demonstrated. The ratio $R_{active}/R_{meta}$, where $R_{meta} = R_{mu} + \Re(Z_{ref})$, is varied. The mutual inductance between the metamaterial units and the loop antenna is 0.3 $\mu$H, the self-inductance of a metamaterial unit is 30 nH, and the unit resistance is 0.1 $\Omega$. As we can see in the figure, as the negative resistance varies, the metamaterial gain can be adjusted from 1 to 30 dB.

In Fig. 10 the effects of node density on empty cell and average source-destination distance are investigated. The network edge length $l_s$ is 120 m and sub-cube edge length is 6 m. The node density is set to 0.04. As estimated in (12), the average distance between each pair of source and destination is 84.8 m, which matches well with the numerical simulation results. It should be noted that the average distances between the sources and the associated destinations are almost not affected by the node density. As a result, the average distance in the figure is nearly a straight line. Also, when the node density is higher than 0.02, empty cells have very low percentage which satisfies the assumption of this paper.

Next, the effects of the reconfigurable gain on link budget and communication range are discussed. We consider the transmitter and the receiver have the same metamaterial gain and vary the value of the gain from 1 to 30 dB. As shown in Fig. 11, as the gain increases the communication range becomes larger which creates more interference to adjacent nodes and the maximum communication range is 40 m. When the gain becomes larger than 10 dB, the link budget becomes saturated because of the strong coupling, i.e., $\omega^2 M^2$ becomes

dominant on the denominator of (8). Then, the randomly distributed relays are considered in Fig. 12. Here, three different metamaterial gain control strategies are considered. In the first strategy, all the nodes use the minimum metamaterial gain, i.e., $\alpha_{gain} = 1$, and the link budget is very high. As a result, using the minimum gain can only achieve very limited communication range. Then, in the second strategy, all the nodes blindly use the maximum metamaterial gain and the link budget is relatively small. The communication range is very long and it can reach 20 cells away. The third strategy uses (11) to determine the metamaterial gain. As we can see in the figure, the link budget performance is very close to the maximum gain strategy but each node smartly control its gain based on the received signal strength from the previous node. Then, we consider the required data rate is 10 kbps and the bandwidth is 1 kHz. According to the Shannon capacity, the required SNR should be larger than 30 dB. Since the transceiver has small resistance, the background noise is dominant which is 120 dBm. $\hat{L}_{max}$ is set as 100 dB and the transmission power is 10 dBm. For the interference area, $\Delta$ is set to 1.

The network delay and capacity are investigated by implementing the proposed MAC protocol and measure the delay from each source to the associated destination. The network load is considered as the density of transmitting sources $\lambda_{sc}$, i.e., if there are many sources having packets to transmit, the network load is high. The node density is set as 0.04 and the maximum relay number for one hop is 5 for $M^2I$ network. All other parameters are the same as preceding discussions. As shown in Fig. 13, both $M^2I$ and MI network's average delay increase as the source density increases because of the congestion. Moreover, the delay of $M^2I$ network is around half of MI network's delay, which is a significant improvement. Also, during the simulation, we find that if the distance

between the source and the destination is within the maximum relay number and all relays are available, the transmission can be done within one time slot. In Fig. 14, the ratio of the maximum number of packets transmitted within one slot to the total number of packets that need to be transmitted is demonstrated. This is also a metric of the network capacity [19]. As shown in the figure, $M^2I$ network and MI network have similar performance but $M^2I$ network has a little higher capacity when the source density is relatively low. The reason is that in $M^2I$ network, the space can be more efficiently utilized when the source density is low because there are more unused space and $M^2I$ network can enlarge its communication range using full-duplex relay, while MI network does not have this capability. When the source density is high, most of the space are utilized, this advantage does not exist. Also, $M^2I$ network have longer communication range and thus its capacity becomes lower than MI network.

## VI. Conclusion

Extreme environment monitoring highly relies on wireless senosr/robot networks. However, existing multi-hop wireless technologies experience high delay, which cannot transmit emergent information and real time control signal timely. In this paper, we propose a low-delay networking strategy by using metamaterial-enhanced magnetic induction ($M^2I$). $M^2I$ demonstrates many desired properties, including (i) reconfigurability by using active input in artificial metamaterial, (ii) full-duplex thanks to the near field magnetic coupling, and (iii) long communication range because of the metamaterial enhancement. In this paper, we for the first time consider these properties of $M^2I$ communication in a wireless network and propose a low-delay networking protocol. The analytical model for the reconfigurable full-duplex $M^2I$ transceiver is derived and the stability and noise are discussed. We provide a strategy for each node in the network to dynamically control its metamaterial gain. Moreover, the analytical network delay model is developed to provide intuitive understanding of the low-delay performance. The numerical results show that using $M^2I$ technology, the delay can be significantly reduced compared with conventional magnetic induction communication. This paper analytically proves the feasibility of the proposed low-delay $M^2I$ network and our future work will focuses on three key challenges: 1) wireless power transmission will be utilized to charge the active metamaterial to make it more compact and self-contained, 2) investigate the scalability of the network protocol and considering more practical issues, 3) implement the proposed protocol in network simulator and real testbed.

## References

[1] J. H. Morecroft, A. Pinto, and W. A. Curry, *Principles of radio communication*. John Wiley & sons, Incorporated, 1921.

[2] Z. Sun and I. F. Akyildiz, "Magnetic induction communications for wireless underground sensor networks," *IEEE Transactions on Antennas and Propagation*, vol. 58, no. 7, pp. 2426–2435, 2010.

[3] E. Shamonina, V. Kalinin, K. Ringhofer, and L. Solymar, "Magneto-inductive waveguide," *Electronics letters*, vol. 38, no. 8, pp. 371–373, 2002.

[4] J. J. Sojdehei, P. N. Wrathall, and D. F. Dinn, "Magneto-inductive (MI) communications," in *OCEANS, 2001. MTS/IEEE Conference and Exhibition*, vol. 1. IEEE, 2001, pp. 513–519.

[5] H. Guo, Z. Sun, and P. Wang, "Multiple frequency band channel modeling and analysis for magnetic induction communication in practical underwater environments," *IEEE Transactions on Vehicular Technology*, 2017.

[6] K. Kant and A. Pal, "Internet of perishable logistics," *IEEE Internet Computing*, vol. 21, no. 1, pp. 22–31, 2017.

[7] H. Guo, Z. Sun, J. Sun, and N. M. Litchinitser, "M²I: Channel modeling for metamaterial-enhanced magnetic induction communications," *IEEE Transactions on Antennas and Propagation*, vol. 63, no. 11, pp. 5072–5087, 2015.

[8] H. Guo, Z. Sun, and C. Zhou, "Practical design and implementation of metamaterial-enhanced magnetic induction communication," *IEEE Access*, vol. PP, no. 99, pp. 1–1, 2017.

[9] R. W. Ziolkowski and A. D. Kipple, "Application of double negative materials to increase the power radiated by electrically small antennas," *IEEE Transactions on Antennas and Propagation*, vol. 51, no. 10, pp. 2626–2640, 2003.

[10] D. R. Smith, J. B. Pendry, and M. C. Wiltshire, "Metamaterials and negative refractive index," *Science*, vol. 305, no. 5685, pp. 788–792, 2004.

[11] G. Oliveri, D. H. Werner, and A. Massa, "Reconfigurable electromagnetics through metamaterials: a review," *Proceedings of the IEEE*, vol. 103, no. 7, pp. 1034–1056, 2015.

[12] T. Riihonen, S. Werner, and R. Wichman, "Mitigation of loopback self-interference in full-duplex mimo relays," *IEEE Transactions on Signal Processing*, vol. 59, no. 12, pp. 5983–5993, 2011.

[13] A. Nosratinia, T. E. Hunter, and A. Hedayat, "Cooperative communication in wireless networks," *IEEE communications Magazine*, vol. 42, no. 10, pp. 74–80, 2004.

[14] I. Krikidis, H. A. Suraweera, P. J. Smith, and C. Yuen, "Full-duplex relay selection for amplify-and-forward cooperative networks," *IEEE Transactions on Wireless Communications*, vol. 11, no. 12, pp. 4381–4393, 2012.

[15] S. Kisseleff, B. Sackenreuter, I. F. Akyildiz, and W. Gerstacker, "On capacity of active relaying in magnetic induction based wireless underground sensor networks," in *Communications (ICC), 2015 IEEE International Conference on*. IEEE, 2015, pp. 6541–6546.

[16] S. E. Sussman-Fort and R. M. Rudish, "Non-foster impedance matching of electrically-small antennas," *IEEE Transactions on Antennas and Propagation*, vol. 57, no. 8, pp. 2230–2241, 2009.

[17] G. Fu and S. Sonkusale, "Broadband energy harvesting using a metamaterial resonator embedded with non-foster impedance circuitry," *arXiv preprint arXiv:1411.0662*, 2014.

[18] E. Ugarte-Munoz, S. Hrabar, D. Segovia-Vargas, and A. Kiricenko, "Stability of non-foster reactive elements for use in active metamaterials and antennas," *IEEE Transactions on Antennas and Propagation*, vol. 60, no. 7, pp. 3490–3494, 2012.

[19] M. J. Neely and E. Modiano, "Capacity and delay tradeoffs for ad hoc mobile networks," *IEEE Transactions on Information Theory*, vol. 51, no. 6, pp. 1917–1937, 2005.

[20] P. Gupta and P. R. Kumar, "The capacity of wireless networks," *IEEE Transactions on Information Theory*, vol. 46, no. 2, pp. 388–404, 2000.

[21] M. Franceschetti, O. Dousse, N. David, and P. Thiran, "Closing the gap in the capacity of wireless networks via percolation theory," *IEEE Transactions on Information Theory*, vol. 53, no. 3, pp. 1009–1018, 2007.

[22] S. Toumpis and A. J. Goldsmith, "Large wireless networks under fading, mobility, and delay constraints," in *INFOCOM 2004. Twenty-third AnnualJoint Conference of the IEEE Computer and Communications Societies*, vol. 1. IEEE, 2004.

[23] C. Balanis, *Antenna Theory: Analysis and Design*. Wiley, 2012.

[24] A. Markham and N. Trigoni, "Magneto-inductive networked rescue system (miners): taking sensor networks underground," in *Proceedings of the 11th international conference on Information Processing in Sensor Networks*. ACM, 2012, pp. 317–328.

[25] Z. Sun and B. Zhu, "Channel and energy analysis on magnetic induction-based wireless sensor networks in oil reservoirs," in *Communications (ICC), 2013 IEEE International Conference on*. IEEE, 2013, pp. 1748–1752.

[26] S.-C. Lin, I. F. Akyildiz, P. Wang, and Z. Sun, "Distributed cross-layer protocol design for magnetic induction communication in wireless underground sensor networks," *IEEE Transactions on Wireless Communications*, vol. 14, no. 7, pp. 4006–4019, 2015.

[27] E. W. Weisstein, "Hypercube line picking," *Delta*, vol. 11, p. 12, 2000.

[28] X. Xie and X. Zhang, "Does full-duplex double the capacity of wireless networks?" in *INFOCOM, 2014 Proceedings IEEE*. IEEE, 2014, pp. 253–261.